On the Location of Conical Intersections in CH_2BrCl Using MS-CASPT2 Methods

Tamás Rozgonyi

Institute of Structural Chemistry, Chemical Research Center, Hungarian Academy of Sciences, 1025 Budapest, Pusztaszeri út 59-67, Hungary

Leticia González*

Institut für Chemie und Biochemie, Takustrasse 3, Freie Universität Berlin, 14195 Berlin, Germany

Received: December 9, 2005; In Final Form: June 22, 2006

Multiconfigurational second-order perturbation theory has been employed to calculate two-dimensional potential energy surfaces for the lowest low-lying singlet electronic states of CH_2BrCl as a function of the two carbon−halogen bonds. The photochemistry of the system is controlled by a nonadiabatic crossing occurring between the $\tilde{A}$ and $\tilde{B}$ bands, attributed to the b^1A' and c^1A' states, which are found almost degenerate and forming a near-degeneracy line of almost equidistant C−Br and C−Cl bonds. A crossing point in the near-degeneracy line is identified as a conical intersection in this reduced two-dimensional space. The positions of the conical intersection located at CASSCF, single-state (SS)-CASPT2, and multistate (MS)-CASPT2 levels of theory are compared, also paying attention to the nonorthogonality problem of perturbative approaches. To validate the presence of the conical intersection versus an avoided crossing, the geometrical phase effect has been checked using the multiconfigurational MS-CASPT2 wave function.

1. Introduction

Conical intersections (CoIn) are photochemical funnels which allow radiationless transitions between electronic excited states.[1] They occur when at least two potential energy surfaces (PESs) intersect. At the intersection, the two surfaces are degenerate, and a molecule can cross from one electronic state to another. Because the time scale on which a transition through a CoIn occurs is only of a few tens of femtoseconds (fs), as demonstrated by femtosecond laser technology and time-resolved spectroscopy, CoIns are the fastest way for an electronically excited molecule to relax back to the ground state or to a lower-lying electronic state. Until recently, CoIns were thought to be a curiosity; over the past years, it has been established that CoIns are ubiquitous. The high photostability of our genetic code is attributed to CoIns; light harvesting, vision, and a variety of essential upper atmospheric processes involve CoIns; and plenty of organic and inorganic molecules undergo CoIns upon ultraviolet (UV) irradiation. In all cases, the CoIn plays an important mechanistic role in the spectroscopy, photochemistry, and chemical kinetics of such processes.

CoIns can be classified according to different criteria,[1] for instance, the role that symmetry plays in their existence. A CoIn is *symmetry-required* when the intersection occurs between two degenerate electronic excited states that belong to the same irreducible representation. An example[1] is the Jahn−Teller intersection between the two E states in C_{3v} symmetry of Na_3. Opposed to symmetry-required CoIns, *accidental intersections* are those where symmetry does not play a role. Here, one can distinguish between *accidental symmetry allowed* and *same symmetry* CoIns. The former corresponds to intersections that occur in a coordinate subspace where the two electronic states have different symmetry, and hence, they may cross freely. The latter refer to intersections between PESs of the same symmetry. According to the noncrossing rule,[2] CoIns between states of the same symmetry are permitted in a space of dimension $\mathcal{N}-2$, the so-called seam space, where $\mathcal{N}$ is the number of internal degrees of freedom ($3N - 6$). Thus, in diatomics, only states of different symmetry can cross, and states of same symmetry lead to an avoided crossing. In polyatomics, however, the noncrossing rule fails, in the sense that states of any symmetry are allowed to cross at any point of the $\mathcal{N}-2$ seam space, as pointed out by Teller[3] in 1969, and largely demonstrated in the last years by many advances in computational photochemistry; see, for instance, refs 4 and 5. The lowest-energy point of the seam space or minimal point of the crossing seam (MXS) is normally referred to as the CoIn (although it is simply the lowest CoIn of the crossing seam).

Despite their omnipresence, CoIns (or MXS) are difficult to predict and locate. At a CoIn, the Born−Oppenheimer approximation breaks down, making it nontrivial to compute the properties of the system with standard quantum chemical methods. Several methods have been proposed to search for the degenerate points.[4,6−10] For instance, Haas, Zilberg, and coworkers[10] exploit the use of elementary reaction coordinates and the phase change rule to find a CoIn between the ground and lowest electronically excited states. The geometrical phase effect, proved first by Longuet-Higgings,[11] states that, if the wave function changes sign when adiabatically transported round a loop in the nuclear configuration, then the loop must contain an odd number of CoIns. Consequently, given a loop for which the adiabatic wave function changes sign once, the loop contains a single CoIn. Therefore, one can construct a loop using, for instance, three points in the electronic ground state, for example, two reactants and one product; and by using elementary reaction coordinates, it is possible to find the point of degeneracy where the phase changes only once between two points.[10] We note that this method, to our knowledge, has not been applied to locate CoIns between different electronically excited states.

* Corresponding author. E-mail: leti@chemie.fu-berlin.de.

10.1021/jp057199s CCC: $33.50
Published on Web 08/05/2006

Moreover, this method, as well as others (e.g., refs 4, 7, and 8), relies on the use of complete active space self-consistent field (CASSCF)[12,13] or multireference configuration interaction (MRCI) wave functions. Recently, Serrano-Andrés et al. have addressed the issue of computing CoIns using single-state and multistate multiconfigurational second-order perturbation theory (single-state SS-CASPT2 and multistate MS-CASPT2) in a number of test cases.[14] In their paper, they illustrate the difficulties in obtaining correct solutions at SS-CASPT2 and MS-CASPT2 levels, and furthermore, even if it has no mathematical basis, they suggest a pragmatic criterion to distinguish a CoIn from an avoided crossing: namely, in a CoIn, the energy difference between the two states should be smaller than 2 kcal/mol. As will be discussed later, this procedure is not straightforward if the PESs are close in energy in a large region of the space.

This paper addresses the question of finding an accidental-same-symmetry CoIn between the two low-lying electronically excited states of a model halomethane, CH_2BrCl. The photochemistry of halomethanes (CH_2XY) has received a lot of attention because of its fundamental role in ozone depletion from the earth's ozone layer.[15,16] When halomethanes absorb ultraviolet (UV) radiation, they are excited to various repulsive states where an electron is promoted from a lone-pair orbital of the halogen to a carbon−halogen antibonding orbital, n(Y) → σ^*(C−Y), leading to C−Y dissociation. The question of whether C−Y or C−X bond-selective dissociation is possible has also been extensively addressed, both theoretically[17,18] and experimentally.[19−23] Different investigations[20,21,24−26] have revealed that the UV photodissociation of these model compounds is largely dominated by nonadiabatic effects between the n(X) → σ^*(C−X) and n(Y) → σ^*(C−Y) states. According to the spectroscopic notation of Herzberg,[27] these transitions form the $\tilde{A}$ and $\tilde{B}$ bands; accordingly, the electronic ground state conforms to the $\tilde{X}$-band. For the sake of consistency with previous publications,[28,29] we prefer to refer to these states as a^1A', b^1A', and c^1A' states, meaning the $\tilde{X}^1A'$, $\tilde{A}^1A'$, and $\tilde{B}^1A'$ states, respectively.

Interested in the photodissociation mechanism of halomethanes, we have recently characterized[28] the vertical excitations of CH_2BrCl and computed one-dimensional (1D) potential energy cuts along both dissociation channels, C−Br and C−Cl, for the electronic ground state and the lowest eight singlet excited states[29] using the MS-CASPT2 method. As we showed in ref 28, the usage of MS-CASPT2 is mandatory due to the strong Rydberg-valence mixing found at CASSCF and SS-CASPT2 levels of theory at the equilibrium geometry. Below the first Rydberg state, MS-CASPT2 predicted four valence states corresponding to either n(Br) → σ^*(C−Br) or n(Cl) → σ^*(C−Cl) transitions in good agreement with the UV spectrum measured by Orkin et al.[30]

Inspection of the b^1A' and c^1A' potential energy curves along the C−Br and C−Cl reaction coordinates[29] indicated the presence of a curve crossing between these two states. To understand how the photoproducts CH_2Br and CH_2Cl are formed, the crossing found at d(C−Cl) = 1.90 Å in the 1D potential was diabatized, and exploratory quantum dynamical simulations were performed indicating halogen fragmentation in less than 100 fs.[29] This preliminary study cannot account, however, for the bifurcation the excited wave packet would follow after going through a CoIn. A previous attempt to predict the direction the excited wave packet follows after excitation was carried out by Takayanagi et al. fitting 2D model PES to spectroscopic data.[25] These model surfaces[25] are, however, not a good approximation for the c^1A' state, since they do not include the effects of several crossings between this and the neighboring adiabatic states out of the Franck−Condon region. In addition, the analytic formula used to describe the crossing between the b^1A' and c^1A' states is qualitatively not correct, since it does not reflect the fact that in this system the noncrossing rule allows two neighboring potential surfaces to cross at a certain point. It is for that reason that we have undertaken the task of calculating 2D PESs and locating the crossing point for the b^1A' and c^1A' states with the help of high-level ab initio computations. This is the aim of the present paper. Determination of the nonadiabatic couplings and the obtainment of regularized diabatized states[31] for a same-symmetry CoIn, as well as 2D dynamical simulations, will be the subject of a subsequent publication. Note that, because we are reduced to two active coordinates, the obtained crossing point does not correspond to the lowest CoIn or to the MXS, but to some point in the $\mathcal{N}-2$ seam space. However, the two chosen coordinates represent the most important reaction coordinates in the system after photoexcitation, and with this assumption in mind, the located CoIn will be the accessible leaking point in the first steps of the reaction.

The paper is organized as follows. Section 2 describes the computational details. Section 3 presents a brief description of the conditions required to find a CoIn, and section 4 presents the results of the 2D PES for the b^1A' and c^1A' states and its CoIn. Finally, section 5 concludes.

2. Computational Details

2.1. Electronic Structure Calculations. All calculations have been done within C_s symmetry. We recall from ref 28 that the nature of the transitions of A′ and A″ symmetry is very similar due to the near-degeneracy of the molecular orbital lone pairs, and most of the A′ excitations are more intense than the A″ counterparts. Therefore, we focus exclusively on the A′ states. Moreover, intersystem crossing is not competitive in the time scale in which dissociation takes place (ca. 100 fs), so triplet states are not taken into account. The PES for the electronic ground and low-lying singlet excited states of A′ symmetry have been calculated starting from the equilibrium geometry of CH_2BrCl, that has been obtained at the MP2(fc)/6-311+G(d,p) level of theory.[28] The optimized parameters are r(C−Cl) = 1.764 Å, r(C−Br) = 1.933 Å, r(C−H) = 1.086 Å, θ(BrCCl) = 113.5°, θ(HCH) = 111.2°, and θ(HCBr) = 107.3°. The chosen reaction coordinates are the bond lengths d(C−Br) and d(C−Cl), which are varied over the ranges 1.65−6.0 and 1.45−6.0 Å, respectively; the other geometrical parameters were kept fixed at their equilibrium values.

The energies have been obtained by means of multiconfigurational second-order perturbation theory. The reference wave function, which provides molecular orbitals, is initially determined from a state average CASSCF (SA-CASSCF) calculation.[12] The dynamical correlation is then provided by the subsequent multistate second-order perturbation theory treatment (MS-CASPT2). Generally, contracted basis sets of the type atomic natural orbitals (ANO-L) were used for C, H, and Cl atoms:[32] (14s9p4d)/[4s3p2d] for the C atom, (8s4p)/[3s2p] for the H atoms, and (17s12p5d)/[5s4p2d] for the Cl atom. For the Br atom, the relativistic core potential AIMP (9s8p4d)/[3s4p2d] (effective atomic number Z = 7.0) was employed.[33] Additionally, the basis sets for C, Cl, and Br have been augmented with an extra set of 2s′2p′1d′ diffuse functions,[34] to describe Rydberg states.

The active space used in the SA-CASSCF calculation consisted of 12 electrons correlated in 12 orbitals, including the main σ, σ^*(C−X) orbitals (X = Br, Cl), the nonbonding halogen n orbitals and Rydberg orbitals; further details can be

found in ref 28. Since the inclusion of dynamical correlation at the CASPT2 level can drastically alter the order of states with respect to their order at the CASSCF level, it is necessary to include a sufficient number of states in the SA-CASSCF wave function to guarantee that no low-lying state is missing at the CASPT2 level. In the present case, 11 roots of A′ symmetry are necessary to describe correctly the low-lying valence states of CH_2BrCl at the equilibrium geometry.[28] At larger internuclear distances, the Rydberg states disappear, and thus, less roots could be used;[29] however, for the sake of consistency, 11 roots have been considered over the whole space.

A well-known problem in CASPT2 is the occurrence of intruder states. The best way to remove them is to increase the active space; if this is not possible, the level-shift (LS) technique[35] can be employed. In the present application, the LS was generally taken as 0.3 au except for three ranges (d(C−Br) ≤ 2.5 Å, d(C−Cl) ≤ 1.7 Å), (2.5 Å < d(C−Br) ≤ 5.0 Å, d(C−Cl) ≤ 2.3 Å), and (5.0 Å < d(C−Br)), in which an LS of 0.4 au was required in order to obtain balanced reference weights. To ensure consistency between the points obtained by LS = 0.3 and 0.4 au, the energies of each electronic state within the ranges mentioned above were corrected by the constant value of 0.1 eV.

The MS-CASPT2 approach uses a multidimensional reference space that simultaneously couples different single-state perturbation theory solutions (SS-CASPT2 or simply CASPT2)[36] of the same symmetry, previously included in the SA-CASSCF wave function. In this way, spurious Rydberg-valence mixing can be removed, and near-degeneracies are well-described.[37] This latter feature is very important for a correct description of avoided and especially real crossings, such as, e,g., a CoIn.

All the MS-CASPT2/CASSCF calculations were carried out using either the *MOLCAS 5.0* or *6.0* quantum chemistry software.[38]

2.2. Interpolation. The 2D potential surfaces were obtained by fitting a 2D cubic spline for the ab initio data computed in an irregular mesh. The range of 1.65 Å ≤ d(C−Br) ≤ 6.0 Å, 1.46 Å ≤ d(C−Cl) ≤ 6.0 Å, was scanned so that resolution of the ab initio points generally changed from 0.05 Å for small internuclear separations to 0.5 Å for large ones. In the vicinity of the near-degeneracy between the b^1A' and c^1A' states, additional points with finer resolution were calculated. As we show later, the b^1A' and c^1A' states are found to be almost degenerate along a thin region along the line d(C−Br) ≈ d(C−Cl); therefore, the resolution of these additional ab initio points had to be fine in both directions to avoid erroneous kinks for the interpolated region. In the following, we will refer to the line where d(C−Br) ≈ d(C−Cl), as a near-degeneracy line in which a CoIn is located. For practical reasons, the points in this region were chosen such that they lay on nine straight lines, determined by the constant differences, d(C−Br) − d(C−Cl) = 0.06, 0.07, ..., 0.14 Å. We will call these lines L6, L7, ..., L14. Each of these lines contain the points with the minimum-energy separation between the c^1A' and b^1A' states, i.e., each of these lines crosses the near-degeneracy line. The ab initio points lying in each of these lines were first interpolated by one-dimensional cubic splines with 0.01 Å resolution. Then, the original ab initio data points (i.e., all excluding the additional points along the L6, L7, ..., L14 lines) were interpolated by a two-dimensional cubic spline with the same resolution for all three lowest electronic states. Finally, the energy values of the b^1A' and c^1A' states obtained by the interpolation of the original data points were replaced by the corresponding values of the interpolated L6, L7, ..., L14 lines. This method, being suited to the topology of the avoided crossing region, ensured that no erroneous features are presented by the interpolation.

3. The Geometrical Phase Effect in Conical Intersections

To understand the nature of the crossing between two PESs, it is usually assumed that the two involved electronic states are well-separated from the rest of all possible states present on the molecule. Then, it is possible to write the crossing states Ψ_1 and Ψ_2 by a linear combination

$$\Psi_i = \tilde{c}_{i1}\phi_1 + \tilde{c}_{i2}\phi_2 \quad (i = 1, 2) \tag{1}$$

where ϕ_1 and ϕ_2 are the electronic functions which together with the solutions for the rest of the electronic states form a complete orthonormal set. Under this assumption, the Hamiltonian for the two states in question can be written as

$$H = \begin{pmatrix} H_{11} & H_{12} \\ H_{21} & H_{22} \end{pmatrix} \tag{2}$$

According to the noncrossing rule,[39] two electronic states of the same symmetry and multiplicity are allowed to cross at one point of a two-dimensional conformational space. The reason is that the solutions of the secular equation for the above Hamiltonian are degenerate only if both conditions

$$H_{11} = H_{22} \text{ and } H_{12} = H_{21} = 0 \tag{3}$$

are simultaneously fulfilled.[39] It may be assumed that in the immediate neighborhood of the crossing point the matrix elements are linear functions of two independent coordinates x and y of the conformational space and with a proper choice of these coordinates the Hamiltonian can be written in a form, similar to that of ref 40, so that it is diagonal for $x = 0$ and the crossing takes place at $x = y = 0$[39]

$$H \approx \begin{pmatrix} W + mx - ky & -lx \\ -lx & W + mx + ky \end{pmatrix} \tag{4}$$

where W, m, k, and l are constant parameters. Solving the secular equation for this Hamiltonian, the energy difference between the states turns out to be $\Delta E = 2\sqrt{l^2x^2+k^2y^2}$—just as in ref 40. Those points in the x, y conformation space that belong to some constant $\Delta E = 2R$ value are located on an ellipse centered at $x = y = 0$ with the major axis lying on $x = 0$ and $y = 0$. To see the behavior of the wave functions for points on that ellipse, it is worth defining the angle θ by the equations $lx = -R \sin\theta$ and $ky = R \cos\theta$. Note that this definition is also similar to that of ref 40 but more suitable for the present situation (vide infra). Substituting these expressions into eq 4 and solving the Schrödinger equation for the CI coefficients, we obtain

$$\tilde{c}_{11} = \cos\left(\frac{\theta}{2}\right) \quad \tilde{c}_{12} = -\sin\left(\frac{\theta}{2}\right) \tag{5}$$

$$\tilde{c}_{21} = \sin\left(\frac{\theta}{2}\right) \quad \tilde{c}_{22} = \cos\left(\frac{\theta}{2}\right)$$

It can be seen that, as we move along the ellipse around the CoIn, all the coefficients $\tilde{c}_{ij}$ change sign and so do Ψ_1 and Ψ_2, as pointed out in ref 40. This feature, called "geometrical phase effect", can be used to differentiate a real crossing (i.e., a CoIn) from an avoided crossing.

Let us now consider a quasi-two-level system, similar to the one just described, where the two states are calculated within the MS-CASPT2 approach.[14,37] The symmetrized effective

Hamiltonian, H^{eff}, used in the MS-CASPT2 method, can be written as

$$H^{\text{eff}} \approx \begin{pmatrix} E_1^{\text{SS}} & \Delta/2 \\ \Delta/2 & E_2^{\text{SS}} \end{pmatrix} \tag{6}$$

where Δ is the sum of the off-diagonal elements of the Hamiltonian matrix and E_1^{SS} and E_2^{SS} are the energies of electronic states 1 and 2 at the SS-CASPT2 level.[14] The wave function for electronic state p at the SS-CASPT2 level is given by

$$\Psi_p^{\text{SS}} = \Psi_p^{\text{SA-CAS}} + \Psi_p^{\text{pert}} \tag{7}$$

where Ψ_p^{pert} is the first-order wave function for the state p and $\Psi_p^{\text{SA-CAS}}$ is the wave function at the SA-CASSCF level for the electronic state p obtained as

$$\Psi_p^{\text{SA-CAS}} = \sum_i d_{pi}|i\rangle \tag{8}$$

using the $|i\rangle$ notation for the CASSCF reference functions. The solution of the Schrödinger equation with the Hamiltonian given in eq 6, i.e., the MS-CASPT2 wave function Ψ_p^{MS} for the electronic state p can be then written as

$$\Psi_p^{\text{MS}} = \sum_i c_{pi}|i\rangle + \Psi_p^{\text{pert}} \tag{9}$$

The weighted sum of the reference functions on the right-hand side of eq 9 is called the perturbatively modified CASSCF (PMCAS) wave function, and it is different from the SA-CASSCF wave function, since the coefficients c_{pi} are different from the coefficients d_{pi}. For degenerate SS-CASPT2 solutions, Δ is equal to the energy separation ΔE_{MS} between the states at the MS-CASPT2 level. Similarly to the conditions given in eq 3, the states are degenerate at the MS-CASPT2 level only if both $E_1^{\text{SS}} = E_2^{\text{SS}}$ and $\Delta = 0$ conditions are fulfilled simultaneously.[14] Thus, the comparison of SS- and MS-CASPT2 energies is essential when searching for CoIns, as is clearly stated in ref 14: Both solutions, SS-CASTP2 and MS-CASTPT2, should differ by less than 1−2 kcal/mol to consider results accurate. Moreover, to distinguish a CoIn from an avoided crossing, Serrano-Andrés et al.[14] proposed $\Delta E_{\text{MS}} < 2$ kcal/mol as a practical criterion. As will be illustrated later, this criterion is not enough to locate the CoIn for the present molecule, where there is an ample range of geometries with $\Delta E_{\text{MS}} < 2$ kcal/mol. In this case, we suggest investigating the geometrical phase effect as a further tool for proving the presence of a CoIn. By assuming that Ψ_p^{MS} is mainly determined by the first term in eq 9, the analysis of the geometrical phase effect can be done using the configuration-interaction (CI) coefficients c_{pi}. This requires that the reference functions do not change considerably at around the crossing, or in other words, that the change of the SA-CASSCF molecular orbitals in the vicinity of the crossing is negligible.

4. Results and Discussion

4.1. Topology of b^1A' and c^1A' Potential Energy Surfaces. In the following, we analyze the results obtained at the most accurate, MS-CASPT2, level of theory. Differences between results obtained at different levels of theory will be discussed in connection with the surface crossing in section 4.2.

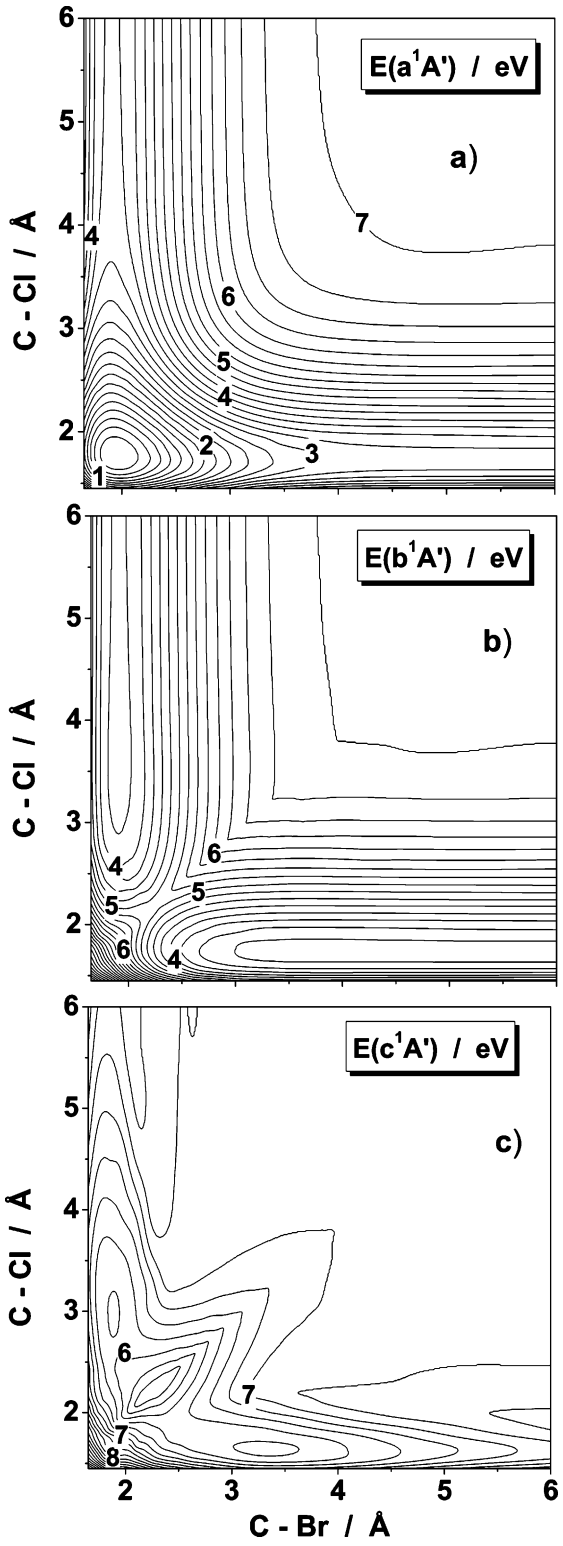

Figure 1. MS-CASPT2 two-dimensional potential energy surfaces. Panels a, b, and c show the potential energy surfaces for electronic states a^1A', b^1A', and c^1A', respectively. The numbers indicate energy values (in eV) measured from the minimum of the electronic ground state a^1A'. The energy separation between the neighboring contour lines is 0.25 eV.

Figure 1 shows the nonrelaxed adiabatic potential energy surfaces for the ground and two lowest electronically singlet excited states computed at the MS-CASPT2 level of theory. The state b^1A' has a saddle point at d(C−Br) = 2.25, d(C−Cl) = 2.19 Å. The vertical potential energy of the b^1A' state at this point is 5.08 eV. At a very close geometry, the c^1A' state has

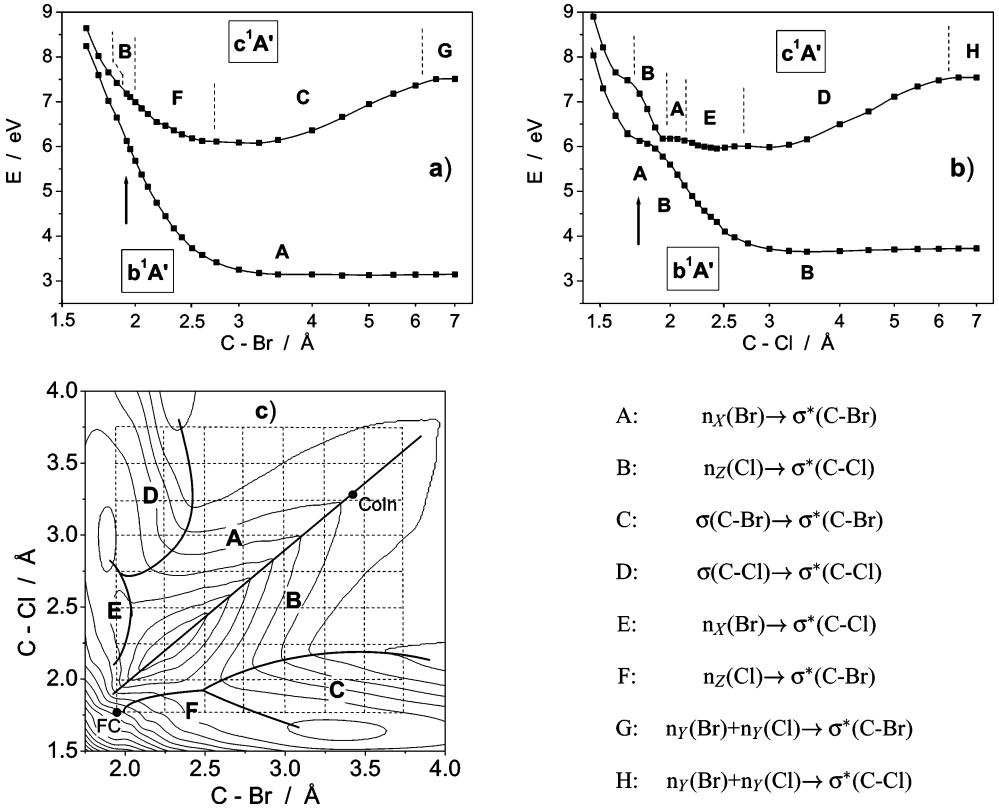

Figure 2. MS-CASPT2 one-dimensional potential energy cuts. Panels a and b show 1D cuts of the 2D potential energy surfaces for the b^1A' and c^1A' states along the C−Br and C−Cl reaction coordinates, with other reaction geometrical parameters fixed to their ground-state equilibrium values. The horizontal axis is in logarithmic scale; the energy is measured from the lowest-energy value of the a^1A' state. The Franck−Condon point is indicated by an arrow in both panels. Points show the calculated ab initio values; solid lines are the corresponding cuts of the 2D splined surfaces. The excitations characterizing the electron structure at different regions are noted by capital letters, whereas the approximate position of the borders of these regions are indicated schematically by dashed lines. Note that only the electron structures in and beyond the Franck−Condon region are indicated. Panel c displays the contour plot of the potential energy of c^1A' state with thin lines. The positions of the Franck−Condon point and that of the CoIn are indicated by the notations FC and CoIn, respectively. The electron configuration was determined in each point of the grid shown by dashed lines. Domains of electronic configurations for the c^1A' state are displayed schematically using bold lines. The excitations, describing the different regions, are noted by the same letters used in panels a and b. The assignment is given next to panel c.

its global minimum, with an excitation energy of 5.27 eV, i.e., the energy gap between the b^1A' and c^1A' at this point is ca. 0.19 eV. As seen in Figure 1c, there exist two additional local minima in the c^1A' potential energy surface: one located at d(C−Br) = 1.89, d(C−Cl) = 2.99 Å, and the other at d(C−Br) = 3.32, d(C−Cl) = 1.65 Å. The corresponding energies are 5.97 and 5.93 eV, respectively.

At large distances, the two lowest states become degenerate, i.e., the energy difference is less than some millielectronvolts. In other words, if d(C−Cl) > 5 Å, $E(a^1A') \approx E(b^1A')$ for any d(C−Br); if d(C−Br) > 5 Å, the $E(a^1A') \approx E(b^1A')$ for any d(C−Cl); and, if both d(C−Br) and d(C−Cl) are greater than 5 Å, then $E(a^1A') \approx E(b^1A') \approx E(c^1A')$.

Figure 2 shows one-dimensional (1D) potential cuts of the 2D PES along C−Br and C−Cl coordinates, keeping the other carbon−halogen distance as well as all the other nondisplayed coordinates at the equilibrium geometry. In agreement with our previously calculated 1D potential energy curves,[29] the first adiabatic excited state is directly dissociative in the C−Br direction (cf. Figure 2a) but also dissociative in the C−Cl direction via the crossing between the c^1A' and b^1A' states (cf. Figure 2b). In the 1D cut along the C−Cl direction (d(C−Br) = 1.93 Å), this crossing takes place at d(C−Cl) = 1.9 Å with an energy gap of 0.37 eV.[29] The adiabatic state b^1A' is less steep in the C−Cl direction than in the C−Br one, indicating preferential C−Br bond fission after excitation to the first electronic excited state, in agreement with experimental observations.[19,22] The b^1A' state is closed for the $CH_2BrCl \rightarrow CH_2 + Br + Cl$ reaction. In contrast, the c^1A' state is closed for both $CH_2BrCl \rightarrow CH_2X + Y$ (X, Y = Br, Cl) directions, but it is "almost" open for the $CH_2BrCl \rightarrow CH_2 + Br + Cl$ reaction, especially if we consider geometry relaxation, which is not taken into account in the present investigations.

4.2. Electronic Structure of the Excited States. To evidence the CoIn (vide infra), it helps to analyze the composition of the wave function describing the adiabatic b^1A' and c^1A' states in the whole coordinate space.

First, let us recall the electronic configuration of CH_2BrCl at equilibrium geometry in the electronic ground state. Placing the C atom at the origin of the coordinate system, with the Br atom on the z axis and the Cl in the xz plane, the closed-shell $^1A'$ ground state corresponds to the $\sigma(C\text{−}Cl)^2\ \sigma(C\text{−}Br)^2\ n_z(Cl)^2\ n_x(Br)^2\ n_y(Cl)^2\ n_y(Br)^2\ \sigma^*(C\text{−}Cl)^0\ \sigma^*(C\text{−}Br)^0$ configuration. At the equilibrium geometry, MS-CASPT2 predicts two valence excited states of A′ symmetry below the lowest Rydberg state at 6.12 and 7.18 eV, respectively, in good agreement with the experimental UV spectrum.[28,30] The corresponding transitions are $n_x(Br) \rightarrow \sigma^*(C\text{−}Br)$ and $n_z(Cl) \rightarrow \sigma^*(C\text{−}Cl)$, respectively.

Figure 2a,b presents the 1D cuts of the two states along the C−Br and C−Cl distances, respectively. In accord with our previous investigations obtained using nine roots,[29] it is found that the lowest adiabatic b^1A' and c^1A' states present a complicated wave function composition, coming from avoided crossings with upper states. Note that only the electron structure

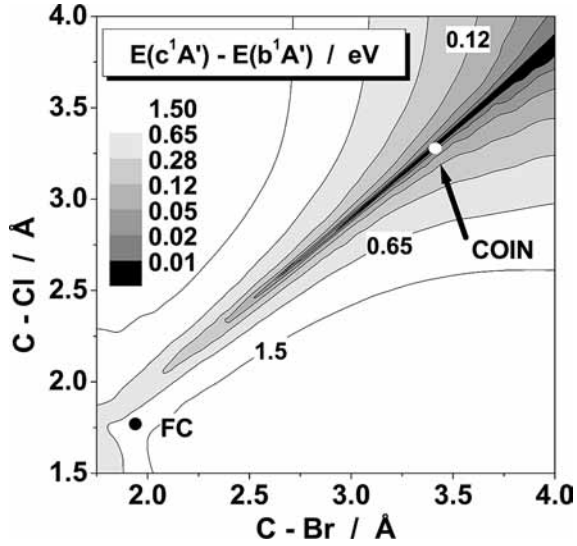

Figure 3. Energy difference between the b^1A' and c^1A' states calculated at the MS-CASPT2 level. The contour levels are increasingly logarithmic. The Franck−Condon point and the position of the conical intersection are indicated by the notations FC and COIN, respectively.

in and beyond the Franck−Condon region are indicated in the figure. The approximate position of the borders between regions of different electron configurations denoted by capital letters is indicated schematically by dashed lines. The electron structure of state c^1A' changes rapidly via avoided crossings as a function of only one C−X distance (X = Br or Cl) when the rest of the coordinates are fixed to their equilibrium values. In contrast, the electron structure of the b^1A' state can be described either by a n_x(Br) → σ^*(C−Br) or n_z(Cl) → σ^*(C−Cl) excitation.

Figure 2c shows the complexity of the c^1A' wave function in 2D. Together with the contours of the c^1A' PES, a rough separation between regions of different electron configurations is indicated by bold lines. We observe that the borders between the different electronic structure regions follow the topology of the surface: The points where the course of the contour lines changes suddenly coincides very well with the meeting points of the regions with different electronic structure. Consequently, the sudden changes of the wave function can be explained as avoided crossings between the different diabatic states which contribute to the adiabatic c^1A' state.

When the distances C−Br and C−Cl change simultaneously, the c^1A' can be described as either n_x(Br) → σ^*(C−Br) or n_z-(Cl) → σ^*(C−Cl) (cf. Figure 2c). The same is true for the b^1A' state. The properties of the crossing between these two states are discussed below.

4.3. The b^1A'/c^1A' Conical Intersection. The energy difference between states b^1A' and c^1A' at the MS-CASPT2 level is displayed in Figure 3. This difference potential surface clearly illustrates that the b^1A' and c^1A' states are almost degenerated along a big region of the d(C−Br) ≈ d(C−Cl) line forming what we defined as a near-degeneracy line. The minimum energy separation between states b^1A' and c^1A' at the MS-CASPT2 level is found at the point d(C−Br) = 3.4 Å and d(C−Cl) = 3.28 Å, with an energy gap ΔE_{MS} = 0.35 meV; therefore, we considered this point to be the location of the CoIn in the 2D subspace.

Most of the CoIns described in the literature are calculated using the CASSCF method, assuming that the location of the degeneracy is the same when dynamical correlation is included but shifted in energy. Because our molecular system shows a large region where two states are very close in energy at the

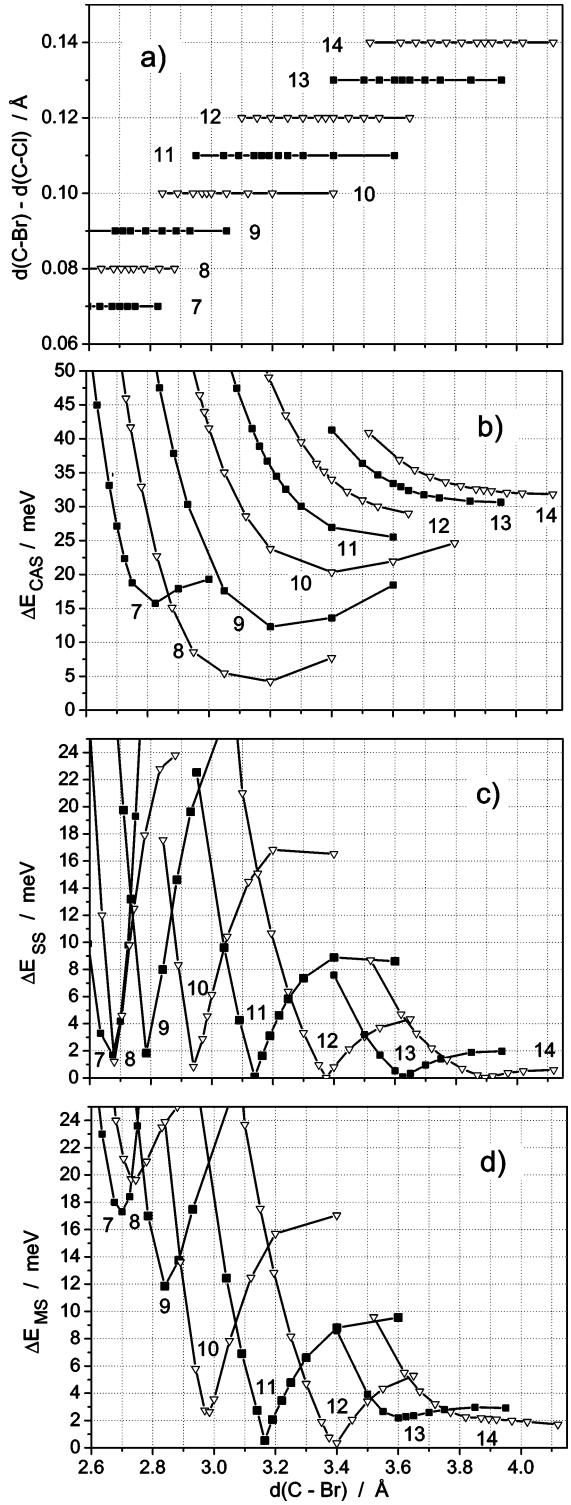

Figure 4. Energy differences around the near-degeneracy line at different levels of theory. Panel a shows the points computed to define the near-degeneracy line at the MS-CASPT2 level. Panels b, c, and d show the $\Delta E = E(c^1A') - E(b^1A')$ values obtained at the SA-CASSCF, SS-CASPT2, and MS-CASPT2 levels of theory, respectively. The numbers indicate the line of constant difference in the bond lengths (in 10^{-2} Å).

MS-CASPT2 level of theory, we found it interesting to analyze the behavior of the PES at different levels of theory, namely, CASSCF, SS-CASPT2, and MS-CASPT2. The results are summarized in Figure 4. The points in the vicinity of the near-degeneracy line are shown in Figure 4a. The points are selected from lines of constant d(C−Br) − d(C−Cl) distances, termed

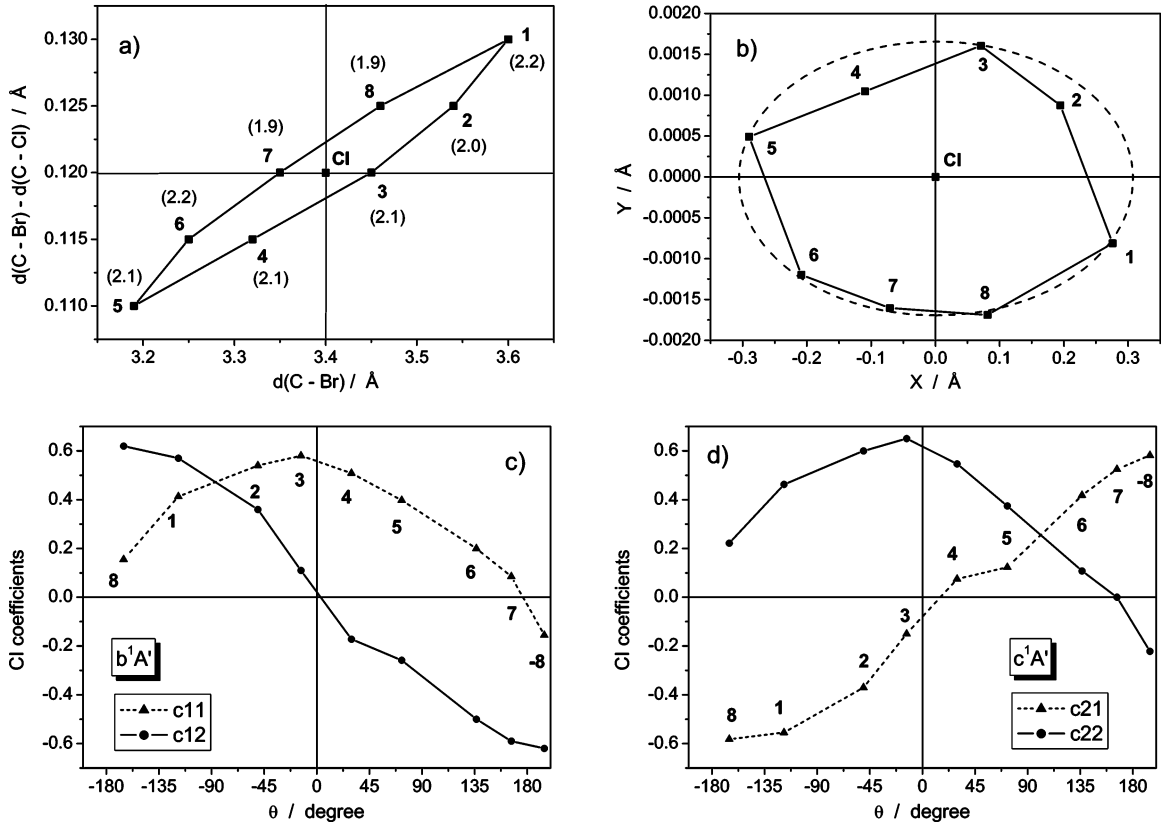

Figure 5. Geometrical phase effect. Panel a shows eight points around the CoIn for similar $\Delta E = E(c^1A') - E(b^1A')$. The indices of the points are shown next to each point with corresponding ΔE (in meV) in parentheses. The CoIn is indicated by "CI". Panel b shows the same points after a coordinate transformation (see text). An ellipse centered in the CoIn was fitted to the points and depicted by dashed lines in the figure. Panels c and d show the two major CI coefficients for the b^1A' and c^1A' states, respectively. The point "−8" is identical to point 8 with reversed coefficient signs. The angles θ are determined using the parameters of the ellipse shown in panel b.

L7, L8, ..., and so forth (see section 2.2). For example, 14 means that, for each point on this line, the d(C−Cl) value is given as d(C−Br) − 0.14 Å.

The $E(c^1A') - E(b^1A')$ energy gap values at the three different levels of theory are presented in Figure 4b−d. The minima of these lines lie at the near-degeneracy line displayed in Figure 3. At the SA-CASSCF level (Figure 4b), the lowest-energy gap, and therefore the CoIn, can be assigned to d(C−Br) = 3.2 and d(C−Cl) = 3.12 Å, slightly different from d(C−Br) = 3.4 and d(C−Cl) = 3.28, obtained at the MS-CASPT2 level. Interestingly, the energy gap at SA-CASSCF is much larger than that obtained using perturbation techniques. Comparison of SS- and MS-CASPT2 energies shows that the degeneracy observed at the SS-CASPT2 level is maintained over a larger range of geometries than for the case of MS-CASPT2 energies, where the degeneracy is restricted to the immediate vicinity of the position d(C−Br) = 3.4 Å, d(C−Cl) = 3.28 Å (cf. Figure 4d). The fact that the profile of L11 and L12 curves is very similar at SS-CASPT2 and MS-CASPT2 levels of theory tells us that the SS-CASPT2 states are orthogonal at these points, confirming the realiability of the CoIn position. Note that, with the SS-CASPT2 method alone, one would not be able to assign the CoIn. Because the energy gap at the minimum of L12 is the smallest, we assigned the CoIn to this point. At this geometry, the (asymmetric) off-diagonal MS-CASPT2 Hamiltonian elements[14] between the b^1A' and c^1A' states, H_{12} and H_{21}, are 0.45 and 0.38 kcal/mol, i.e., relatively similar and very small, indicating that the SS-CASPT2 solutions are already orthogonal, as confirmed by the MS-CASPT2 solution. The average (symmetric) off-diagonal MS-CASPT2 Hamiltonian[14] Δ is then computed as 0.07 kcal/mol; note that this splitting due to the orthogonality of the states also takes into account the interaction between the other states, besides b^1A' and c^1A'.

Figure 4, as well as Figure 3, shows that the qualitative criterion of $\Delta E < 2$ kcal/mol (87 meV) to locate a CoIn[14] cannot be used in CH_2BrCl, because the energy gap is smaller than this value all along the near degeneracy line for d(C−Br) > 2.4 Å. Moreover, the two involved states become degenerate for simultaneously diverging internuclear separations; therefore, the criterion of minimum-energy difference alone does not suffice to locate a CoIn. Instead, we suggest proving the existence of a real CoIn by investigating the geometrical phase effect (GPE).

To illustrate the GPE, the configuration interaction (CI) coefficients defined in eq 9 have been investigated and compared to the expected behavior—described in section 3. Prerequisites for this analysis are that the two electronic states in question are separated from the rest of the states and that the change of the reference functions in the investigated region is negligible. The b^1A' and c^1A' states are energetically well separated from the rest of the electronic states at around the CoIn. At the position of the CoIn, both the energy gap between states c^1A' and d^1A' and the gap between states a^1A' and b^1A' are ca. 0.3 eV, which is orders of magnitude larger than the energy gap between the crossing states at around the CoIn.

Furthermore, we have analyzed the electronic structure of the reference functions, i.e., the SA-CASSCF molecular orbitals involved in the two crossing states, for each point around the CoIn (see later). We found that the deviation in the main atomic orbital coefficients of the active molecular orbitals is typically much less than 10%. Likewise, the deviation of the bond-lengths

of the selected points around the CoIn is also less than 10%. Consequently, the change of the reference functions can be neglected.

To make the investigation of the GPE easier, the original coordinate system (d(C−Br), d(C−Cl)) was shifted into the CoIn and was rotated by 43.7°. The new coordinate system, denoted (X, Y), suits the present situation inasmuch as the near-degeneracy line lies on axis X, with the CoIn in the origin, as it was assumed in section 3. We select ab initio points with constant $\Delta E_{MS} \approx 2$ meV energy gap to fit an ellongated ellipse with the origin in the CoIn. The selected points and the fitted ellipse in the transformed coordinate system are presented in Figure 5a,b, respectively. The ratio of the main axis of the ellipse gives the ratio of parameters k and l (cf. section 3) as $k/l = 183.5$.

As is typical for multiconfigurational wave functions at each selected geometry, the wave function is composed of more than two electronic configurations. There are, however, two configurations for which either one or the other had the CI coefficient with the largest absolute value for all the selected conformations at around the CoIn. Therefore, these configurations can be regarded as the main configurations, and thus to illustrate the GPE, we have considered only the coefficients of these two configurations. The SA-CASSCF reference functions belonging to these coefficients can be assigned as $|1\rangle$: n_z(Cl) → σ^*(C−Cl) and $|2\rangle$: n_x(Br) → σ^*(C−Br). The corresponding CI coefficients, c_{pi} (p, $i = 1, 2$) (cf. eq 9) as a function of θ are presented in Figure 5c,d; θ is computed as arctan($-lx/ky$) from the (x, y) coordinates of the selected points according to the definition of θ in section 3. The behavior of the CI coefficients for the b^1A' and c^1A' states is as predicted by eq 5, proving the existence of a real CoIn in the reduced 2D subspace. It is gratifying to see that the deviation of the curves from the exact sinusoidal shapes is rather small. The norm $|c_{i1}|^2 + |c_{i2}|^2$ is less than the unity because other configurations in the PMCAS wave function have been neglected; yet, their CI coefficients have been also investigated, finding that they also change sign once for a loop around the CoIn, as expected for a CoIn.

5. Conclusion

Two-dimensional nonrelaxed potential energy surfaces for the three lowest singlet electronic states of A′ symmetry were computed for the CH_2BrCl molecule as a function of the two carbon−halogen bond lengths, corresponding to the two primary photodissociation pathways of the molecule. The potential surfaces were determined at the MS-CASPT2 level of theory due to the inability of variational methods to describe correctly valence and Rydberg states. A global minimum of the c^1A' surface was located at d(C−Br) = 2.24 and d(C−Cl) = 2.20 Å. Along the line of d(C−Br) ≈ d(C−Cl), the b^1A' and c^1A' states are very close in energy. Along this line, a CoIn at d(C−Br) = 3.40, d(C−Cl) = 3.28 Å is located using very fine resolution and MS-CASPT2 energies. The location of the CoIn was also investigated using the CASSCF and SS-CASPT2 approaches. The position of the CoIn at MS-CASPT2 can also be found at the SS-CASPT2 level, showing that at the CoIn geometry the SS-CASPT2 wave functions are already orthogonal.

CoIns determined by numerical procedures are never exactly degenerate and CoIns arising from two states of the same symmetry are difficult to anticipate (Yarkony following Berry[42] notation termed such CoIn diabolical[4,43]). Therefore, in these cases, the verification of the GPE is the only evidence of the existence of a CoIn. Here, we employed the multiconfigurational second-order perturbation wave functions to follow the GPE. To our knowledge, this is the first time that the GPE has been investigated numerically using the MS-CASPT2 procedure between two electronically excited states of the same symmetry, although this procedure has been reported many times using SA-CASSCF and MRCI wave functions (see, for instance, refs 4 and 41).

Since the energy gap between b^1A' and c^1A' states is extremely small along a large region of the space, even before the CoIn, it is an open question whether the CoIn really does take part in the photodissociation dynamics, especially in the $CH_2BrCl + h\nu \rightarrow CH_2Br + Cl$ reaction, or is it the part of the near-degenerated region, well before the CoIn and closer to the Franck−Condon region, which plays the crucial role in the nonadiabatic photochemistry of CH_2BrCl. Wave packet propagations to investigate the dynamic behavior of the system are in progress.

Acknowledgment. We are grateful to Prof. H. Köppel for enlighting discussions about the theory of conical intersections and to Dr. Serrano-Andrés for helpful comments on the usage of MS-CASPT2. L.G. thanks the "Berliner Programm zur Förderung der Chancengleichheit für Frauen in Forschung und Lehre" and the SFB 450 "Analysis and Control of Ultrafast Photoinduced Reactions" for travelling financial support. All quantum chemical calculations have been performed on the HP-UX servers of the Theoretische Chemie group at the Freie Universität Berlin.

References and Notes

(1) *Conical Intersections: Electronic Structure, Dynamics and Spectroscopy*; Domcke, W., Yarkony, D. R., Köppel, H., Eds.; World Scientific: Singapore, 2004.
(2) von Neumann, J.; Wigner, E. *Phys. Z.* **1929**, *30*, 467.
(3) Teller, E. *Isr. J. Chem.* **1969**, *7*, 227.
(4) Yarkony, D. R. *Rev. Mod. Phys.* **1996**, *68*, 985.
(5) Bernardi, F.; Olivucci, M.; Robb, M. A. *Chem. Soc. Rev.* **1996**, *25*, 321.
(6) Köppel, H.; Domcke, W.; Cederbaum, L. S. *Adv. Chem. Phys.* **1984**, *57*, 59.
(7) Ben-Nun, M.; Martinez, T. *Chem. Phys.* **2000**, *259*, 237.
(8) Blancafort, L.; Ogliaro, F.; Olivucci, M.; Robb, M. A.; Bearpark, M. J.; Sinicropi, A. In *Computational Investigation of Photochemical Reaction Mechanisms*; Marcel Dekker: New York, 2005; pp 31−110.
(9) Lischka, H.; Dallos, M.; Szalay, P. G.; Yarkony, D. R.; Shepard, R. *J. Chem. Phys.* **2004**, *120*, 7322.
(10) Yehuda, H.; Cogan, S.; Zilberg, S. *Int. J. Quantum Chem.* **2005**, *102*, 961.
(11) Longuet-Higgings, H. C. *Proc. R. Soc. London, Ser. A* **1975**, *344*, 147.
(12) Roos B. O. In *Advances in Chemical Physics; Ab initio Methods in Quantum Chemistry II*; Lawley, K. P., Ed.; Wiley: Chichester, 1987; p 399.
(13) Roos, B. O.; Taylor, P. R. *Chem. Phys.* **1980**, *48*, 157.
(14) Serrano-Andrés, L.; Merchán, M.; Lindh, R. *J. Chem. Phys.* **2005**, *122*, 104107.
(15) *Chemistry and Radiation Changes in the Ozon Layer*; Zerefos, C. S., Isaksen, I. S. A., Ziornas, I., Eds.; Kluwer: Dordrecht, 2001.
(16) *The Chemistry of Atmospheres*; Wayne, R. P., Ed.; Oxford University: New York, 1991.
(17) Abrashkevich, D. G.; Shapiro, M.; Brumer, P. *J. Chem. Phys.* **2002**, *116*, 5584.
(18) Liu, K.; Zhao, H.; Wang, C.; Zhang, A.; Ma, S.; Li, Z. *J. Chem. Phys.* **2005**, *122*, 044310.
(19) Tzeng, W. B.; Lee, Y. R.; Lin, S. M. *Chem. Phys. Lett.* **1994**, *227*, 467.
(20) McGivern, W. S.; Li, R.; Zou, P.; North, S. W. *J. Chem. Phys.* **1999**, *111*, 5771.
(21) Zou, P.; McGivern, W. S.; North, S. W. *Phys. Chem. Chem. Phys.* **2000**, *2*, 3785.
(22) Lee, S.-H.; Jung, Y.-J.; Jung, K.-H. *Chem. Phys.* **2000**, *260*, 143.
(23) Damrauer, N. H.; Dietl, C.; Kramert, G.; Lee, S.-H.; Jung, K.-H.; Gerber, G. *Eur. Phys. J. D* **2002**, *20*, 71.

(24) Zhang, J.; Heller, E. J.; Huber, D.; Imre, D. G.; Tannor, D. *J. Chem. Phys.* **1988**, *89*, 3602.
(25) Takayanagi, T.; Yokoyama, A. *Bull. Chem. Soc. Jpn.* **1995**, *68*, 2225.
(26) Jung, Y.-J.; Park, M. S.; Kim, Y. S.; Jung, K.-H.; Volpp, H.-R. *J. Chem. Phys.* **1999**, *111*, 4005.
(27) *Molecular Spectra and Molecular Structure. III. Electronic Spectra and Electronic Structure of Polyatomic Molecules*; Herzberg, G., Ed.; Van Nostrand Reinhold Company: New York, 1966.
(28) Rozgonyi, T.; Feurer, T.; González, L. *Chem. Phys. Lett.* **2001**, *350*, 155.
(29) Rozgonyi, T.; González, L. *J. Phys. Chem. A* **2002**, *106*, 11150.
(30) Orkin, V. L.; Khamagonov, V. G.; Guschin, A. G.; Huie, R. E.; Kurylo, M. J. *J. Phys. Chem.* **1997**, *101*, 174.
(31) Köppel, H.; Schubert., B. *Mol. Phys.* **2006**, *104*, 1069.
(32) Widmark, P.-O.; Malmqvist, P.-A.; Roos, B. O. *Theor. Chim. Acta* **1990**, *77*, 291.
(33) Barandiarán, Z.; Seijo, L. *Can. J. Chem.* **1992**, *70*, 409.
(34) Kaufmann, K.; Baumeister, W.; Jungen, M. *J. Phys. B: At. Mol. Opt. Phys.* **1989**, *22*, 2223.
(35) Roos, B. O.; Andersson, K. *Chem. Phys. Lett.* **1995**, *245*, 215.
(36) Andersson, K.; Malmqvist, P.-A.; Roos, B. O. *J. Chem. Phys.* **1992**, *96*, 1218.
(37) Finley, J.; Malmqvist, P.-A.; Roos, B. O.; Serrano-Andrés, L. *Chem. Phys. Lett.* **1998**, *288*, 299.
(38) Karlström, G.; Lindh, R.; Malmqvist, P.-Å.; Roos, B. O.; Ryde, U.; Veryazov, V.; Widmark, P.-O.; Cossi, M.; Schimmelpfennig, B.; Neogrady, P.; Seijo, L. *Comput. Mater. Sci.* **2003**, *28*, 222.
(39) Teller, E. *J. Phys. Chem.* **1937**, *41*, 109.
(40) Herzberg, G.; Longuet-Higgins, H. C. *Trans. Faraday Soc.* **1963**, *35*, 77.
(41) Yarkony, D. R. *J. Chem. Phys.* **1996**, *104*, 2932.
(42) Berry, M. V.; Wilkinson, M. *Proc. R. Soc. London, Ser. A* **1984**, *392*, 15.
(43) Yarkony, D. R. *J. Phys. Chem.* **2001**, *105*, 6277.